Monitoring of Femtosecond Laser Micromachining Using Ultra-high Speed Photodiodes: The Effect of Feature Depth on the Optical Process Emission

Kerim Yildirim*[1], Balasubramanian Nagarajan[1], Tegoeh Tjahjowidodo[2], and Sylvie Castagne[1]

[1]*KU Leuven, Department of Mechanical Engineering and Flanders Make@KU Leuven - M&A, Celestijnenlaan 300, 3001 Leuven, Belgium*
[2]*KU Leuven, Department of Mechanical Engineering, Jan Pieter de Nayerlaan 5, 2860, Sint-Katelijne-Waver, Belgium*
**Corresponding author's e-mail: kerim.yildirim@kuleuven.be*

The femtosecond (fs) pulsed laser is a versatile tool to produce microstructures down to a few microns on all kinds of materials including metals, ceramics and polymers. Generally, the topography of the fabricated structures is characterized using ex-situ measurement techniques such as confocal microscopy or white light interferometry, which significantly increases the process cycle time. Besides, it is difficult to control the laser process parameters in real-time with offline characterization methods. To closed loop the fs laser micromachining (FLμM) process, an in-process sensing strategy is required. However, unlike for laser processing with continuous and short-pulsed lasers, the process monitoring for FLμM has not been fully explored. In this work, a monitoring system based on off-axis ultra-high speed photodiodes was integrated and applied to the detection of optical process emissions during FLμM of stainless steel. Three photodiodes, whose specifications are described hereafter, were used. The reflected process radiation passes through a filter, with a specific wavelength range of visible (500-900 nm), laser beam reflection (1030 nm) and infrared (1100-1700 nm), focused onto the photodiode with an amplifier circuit. FLμM of a single line ablation at different pulse energies and scanning passes were performed to study the effect of the feature depth on the off-axis photodiode-based monitoring. In addition, a high-speed spectrometer was implemented in the FLμM working station to capture the spectral distribution of the plasma emission. The characteristics of process optical emission, temporal evolution of the spectrometer and photodiode signals, and the effects from laser machining factors were discussed. The proposed monitoring technique using optical emission-based sensor has the potential to facilitate the process control for femtosecond laser micromachining, which will ultimately result in increased productivity and quality.
DOI: 10.2961/ilmn.2024.03.2009
Keywords: femtosecond laser micromachining (FLμM), ultra-short pulse laser ablation, optical emission sensing, in-situ process monitoring, ultra-high speed photodiodes

1. Introduction

Laser-based tools for micromachining have gained significant attention for the fabrication of small-scale components and devices [1], [2]. Besides, laser-based surface functionalization plays an important role to enhance the surface properties of many products, such as modifying the friction property or tuning the wettability, by changing the surface topography. The development of ultrashort pulse (USP) lasers, which has pulse duration in the range of femtoseconds (10^{-15} s) to picoseconds (10^{-12} s), offers high precision and quality necessary in micromachining applications [3], [4]. The primary benefits of material processing with USP lasers are: i) efficient, rapid, and localized energy deposition; ii) well-defined ablation thresholds [5]; and iii) negligible or minimal thermal damage to the substrate [6], and iv) ability to process almost any material (e.g., metals, ceramics, glass, polymers, etc.) [7]. The machined features are extremely smooth and free of burrs, and the surface is clear of redeposited particles [8]. The industrial use of these laser systems for micromachining continues to grow in relevance across a variety of sectors and applications and has become one of the most essential microfabrication tools [9].

However, the need for tight part tolerances and short cycle times presents new obstacles for laser micromachining. As laser processes are influenced by a variety of machine, workpiece, and environment-related factors, even slight parameter changes might result in components that fall outside of the required tolerances. Therefore, the range of acceptable parameter deviations, also known as the process window, is exceedingly narrow for the fabrication of precision components [10].

To achieve the desired geometry of the processed structure, the optimal processing parameters (e.g., wavelength, pulse energy, pulse duration, pulse repetition rate, beam spot size, focal point, and scanning speed) for the target material should be investigated [11]. Due to the absence of a comprehensive physics-based modelling of complex laser-material interaction involved in fs laser processing, a large set of parameters is typically investigated experimen-

tally [12]. However, trial-and-error experiments are time-consuming and expensive due to the large number of process parameters [13]. In addition, traditional post-characterization techniques, such as X-ray computed tomography (CT), atomic force microscopy (AFM) and scanning electron microscopy (SEM) are time- and cost-intensive, and their implementations are constrained by production scale [14].

During laser-based manufacturing, quality monitoring is essential to ensure the quality and performance of the fabricated parts. Therefore, a monitoring approach to predict the ablation profile as a function of laser parameters is required to decrease processing and characterization time [15]. Sensor-based monitoring provides useful information about the manufacturing process that can serve the dual function of process control and quality monitoring, and will eventually be included into every fully automated production environment. For any sensor to be deployed as a monitoring device, however, a high level of confidence and accuracy in characterizing the manufacturing process is necessary [10]. A proper process monitoring system that was integrated into the manufacturing process is helpful for avoiding expensive end-of-line quality assurance and ensuring the durability of textured parts [16], [17].

The potential of capturing the optical emission (OE) signals from the processing zone has been demonstrated in the literature for different laser material processing applications such as laser powder bed fusion and laser welding which employ continuous wave lasers [18-21]. In recent times, the OE-based monitoring technique have also been adopted for laser micromachining but with longer pulses than USP lasers (typically > 1 nanosecond (ns)) [22], [23].

Photodiodes, which are spatially integrated single-channel detectors, are semiconductor devices that transform light (radiation) into electric current. They are frequently used in laser material processing since they are simple to integrate into various configurations [24]. They can be used to measure light intensities and often have a fast response time, which is essential for monitoring laser material processes [25]. The emitted radiation mostly depends on the process itself (the radiation that is used for monitoring), the processed material (spectral emissivity), the used laser (spectral sensitivity of sensor), and the optics (filters, lenses, fibres, having each a characteristic spectral transmission) [26]. The wavelength range that a photodiode can detect is frequently reduced on purpose via optical filtering. The light that passes through the filter is first detected by the photodiode sensor, then processed by a signal amplifier, and finally visualized on an oscilloscope. By measuring the signal intensity of various spectral bands, it is possible, for instance, to identify certain processing regimes [27].

There are three types of optical radiation signals that typically occur in laser-based manufacturing. The first type involves ultraviolet (UV) and visible (VIS) light wavebands (200–750 nm) for which silicon-based photodiodes are used. The second sort of waveband (1030) corresponds to laser reflection. The third type is infrared (IR) radiation waveband (1100–1700 nm) which is acquired by photodiodes based on germanium (Ge) and indium-gallium-arsenide (InGaAs) [28]. In each sensor category, there are single sensor devices and array sensor devices. Often, single-sensor devices are referred to as "integrative" sensors which can only focus on a limited processing region. This 'integrative' single-sensor system simply monitors the overall radiation emitted by the surface with a defined region of interest (dependent of the area of view). It provides the total amount of radiation captured (i.e., intensity of the recorded radiation and its size), but does not provide spatial information about the radiation as provided by cameras.

Based on the configuration of the photodiodes in the laser processing setup, there exists two categories of photodiode-based process monitoring, namely off-axis and coaxial. Off-axis sensors can be placed relative to the principal laser beam. In this scenario, the sensor observes the process from a different direction and with a different set of optics than those of the primary laser beam. That is to say that the laser beam and the sensor both have their own optical paths. Alternatively, in coaxial configuration, the laser beam and emitted radiation act along the same optical axis or "look" at the process in the same direction or along the same axis.

A comprehensive array of photodiode-based monitoring systems has been developed and demonstrated to monitor long-pulsed laser processing [29-31]. By monitoring laser machining with photodiodes, Gehrke et al. [32] demonstrated a correlation between process emission (visible spectrum) and focus position, laser power, ablated volume and the surface roughness. Park et al. [33] constructed a photodiode monitoring system that detects the plasma created during laser marking which can be used to develop marking-width estimation models. During the high-speed marking operation, the photodiode on the coaxial line was able to precisely record the light emission. Based on the relationship between the laser power, the line width, and the recorded sensor data, statistical regression and artificial neural network models were used to predict the width of laser marking. Zuric et al. [34] demonstrated a system for ns laser-based micromachining process and machine condition monitoring in real-time. By monitoring multiple process emissions (UV, laser back reflection and IR) concurrently, a relationship between the signals and the surface roughness was identified. However, most of the reported works were focussed on longer-pulsed lasers than fs laser which involves thermal-based material removal. There are limited studies on OE-based monitoring of the FLµM process which involve non-thermal ablation mechanisms.

The objective for this work is to demonstrate the utilization of the optical emission method by means of UPDs as a possible candidate for process monitoring of FLµM. In particular, the raw OE signals are processed to extract signal features which are then correlated with the feature depth. By gathering high speed and high-resolution signal amplitude at the same frequency as the laser pulses, monitoring of OE signals during FLµM can qualify for tracking the changes in the process condition. In this manuscript, we report on the utilization of the broad spectral range spectrometer for investigating the specific spectral regions of FLµM process.

2. Materials and Methods

2.1 Materials

In this study, flat samples made of stainless steel has been selected as reference material due to its wide range of applications. Non-polished plates of 316L (Grade 1.4404)

stainless steel with a thickness of 1 mm were used. The samples were cleaned with ethanol before and after FLμM.

2.2 Experimental Setup

The opto-mechanical system used for FLμM consists of the fs laser, optical beam delivery components, a 7-axis (3-linear, 2-rotary, and 2-optical) positioning system and electronic control units. The schematic of the fs laser machine for laser ablation experiments is illustrated in Figure 1. The experiments were performed using a Carbide Yb:KGW fs laser (Light Conversion), which has a pulse duration ranging from 178 fs to 10 ps, 1030 nm wavelength, repetition rate up to 1000 kHz and 20 W maximum average power. The maximum pulse energy of a single pulse is approximately 400 μJ (at 50 kHz). A two-axis galvanometric scanner (Scanlab) is used for a fast and precise positioning of the beam for laser scanning. A beam expander is used to expand beam diameter corresponding to the scanner aperture diameter (20 mm, max), which will further reduce the beam diameter to obtain a 16 μm diameter spot size on the workpiece surface. The magnified laser beam is then carried along the beam path until the scanner. After the laser beam passed through the scanner, it is focused by an F-theta lens (f=125 mm) in the normal incidence onto the sample, which was mounted on a 5-axis motorized air bearing positioning stage (LAB Motion Systems) for precise positioning of the sample. The linear stages have a positioning accuracy and repeatability smaller than 0.3 μm, with a resolution below 0.1 μm. The galvanometric scanner in combination with F-theta lens can produce large scanning fields and rates up to 3000 mm/s, which allows a short processing time.

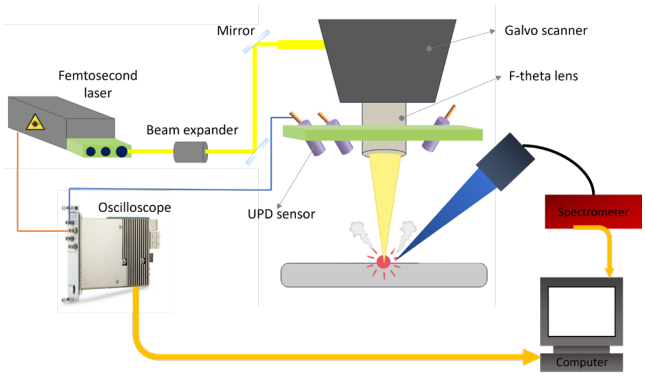

Fig. 1 Schematical representation of the femtosecond laser machine together with integrated spectrometer and UPDs.

Figure 2 shows the experimental setup for detecting the process light generated during laser micromachining by means of the photodiode. The reflected process radiation passes through a filter, with a specific wavelength range of visible – VIS (500-900 nm), laser beam reflection – LBR (1030 nm) and infrared – NIR (1100-1700 nm), focused onto the photodiode with an amplifier circuit. The coating of the bandpass filters is designed to selectively transmit either visible, laser back reflection, and infrared wavelengths according to the photodiode setup. The photodiode consists of a silicon chip specifically designed for the ultraviolet and visible region and an InGaAs chip for the infrared region in terms of spectral sensitivity. The visible process emission is collected via an ultra-high speed Si PIN photodiode (Hamamatsu) with a spectral response range of 350 nm to 1100 nm, a rise time of 1 nanosecond, a cutoff frequency of 100 MHz, and peak sensitivity at 920 nm. It is equipped with a narrow band pass optical filter that has a cut-off wavelength of 750 nm and a central wavelength of 520 nm for selective transmission of the process emission. For specifically detecting the laser beam reflection (1030 nm), an InGaAs PIN photodiode with a rise time of 25 nanoseconds, a cutoff frequency of 60 MHz, and peak sensitivity at 1550 nm was installed behind a bandpass filter (950 – 1100 nm). Another InGaAs PIN photodiode with a longpass filter (1100 nm – 1700 nm) was used to detect the optical emission at near-IR wavelengths. Each photodiode is placed behind a corresponding optical path. The photocurrent output by the photodiode is converted into a voltage signal and amplified using an electrical circuit. This signal is further recorded via an oscilloscope card in the measuring chassis with a sampling rate of 10 MHz. This offers an advantage that the signal can be analysed and evaluated in real-time with the aid of an analysis software (LabVIEW) and that the results can be documented digitally. The obtained data were processed in MATLAB using appropriate statistical analysis and digital filters to reduce the noise.

Table 1 Summary of sensor specifications for optical emission monitoring during FLμM.

Sensor type	Spectral response range	Rise time	Cutoff frequency
Ultra-high speed Si PIN photodiode	350 nm to 1100 nm	1 ns	100 MHz
InGaAs PIN photodiode	950 nm to 1100 nm	25 ns	60 MHz
InGaAs PIN photodiode	1100 nm to 1700 nm	25 ns	60 MHz

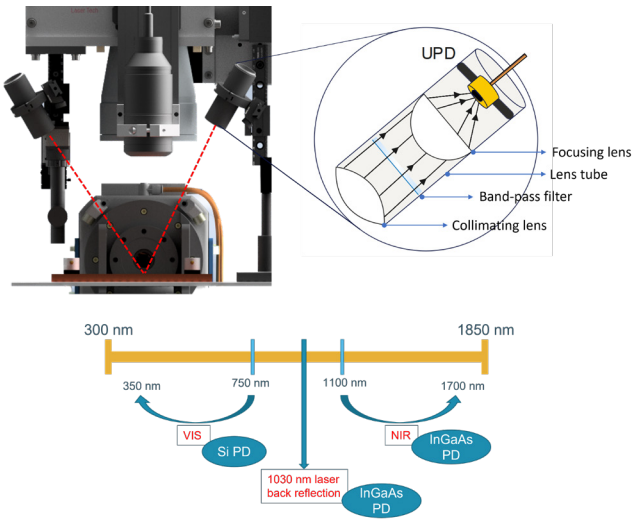

Fig. 2 Illustration of the UPD detectors employed for FLμM monitoring and their corresponding spectral regions.

Due to its compact and robust design, ultrahigh speed photodiodes (UPDs) can be easily and cost-effectively integrated into the laser-based manufacturing setup. With their high light sensitivity and ns-scale response time, UPDs meet the requirements for recording optical process

emissions during FLμM. During the laser scanning, the UPDs move along with the scanner (see, Fig. 1) such that the relative position between the laser irradiation zone and the UPDs always remains constant. Furthermore, as the data volume generated by a photodiode are comparatively small, they can be evaluated online even at the required high sampling rate. All experiments were carried out by irradiating multiple fs laser pulses to create single spot craters or grooves. Each cavity was structured with different laser pulse energies and number of laser scanning passes (Table 1). To investigate the effect of increasing laser pulse energy on the ablation depth and accordingly the UPD signal characteristics, pulse energy ranging from 25 μJ to 100 μJ were tested. The number of pulses ranging from 10 to 100 multiple pulses were analysed. The laser pulse repetition rate was set constant and equal to 200 kHz for all the experimental conditions. Other parameters such as pulse duration (250 fs), scanning (200 mm/s) and jump (200 mm/s) speed between passes were held constant. After laser micromachining, the surface morphology of the ablation crater was characterized with a SEM. The multi-pulse irradiation of spots and single-grooves were executed in 5 different locations as shown in Figure 3.

Table 2 Process parameters used for FLμM.

Parameter	Values/Conditions
Laser pulse energy	25 μJ to 100 μJ
No of pulses	10 to 100 multiple pulses
No of laser scanning passes	1 to 5 passes
Laser pulse repetition rate	200 kHz (constant)
Scanning speed	200 mm/s (constant)
Pulse duration	250 fs (constant)

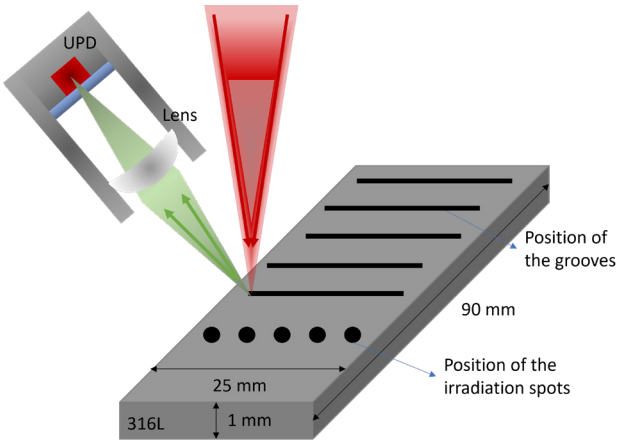

Fig. 3 Schematical illustration of the irradiated spot and groove positions for fs laser ablation experiments.

The Ocean-FX high-speed fibre optic spectrometer (Ocean Insight) was used for the analysis of spectral emission (Figure 1). The spectrometer is responsive from 315 to 1035 nm and is set at a sample rate of 100 Hz, at a resolution ranging from 0.28 to 0.39 nm. The given spectrometer is one of the fastest spectrometer available in the market with its capability of transferring 1 ms spectra continuously. The plasma emission which occurs during the laser ablation of the steel sample in the air at ambient temperature and atmospheric pressure was focused into an optical fibre. The recorded plasma emission spectra were analysed using Oceanview software.

3. Results and Discussion

Fig. 4 represents the spectra acquired for a wavelength range of 315-1035 nm during 15 second micromachining of groove with multiple passes. The intensity peaks can be used as a method to find the most reactive wavelengths and measure only those with different monitoring tool such as single-channel UPD sensors. As seen in Figure 4, the most intense regions in two different zones are as follows: visible region with the peak of 430 nm and laser back reflection region with the peak of 1030 nm. Notably, the intensity at 430 nm remains relatively constant between 4 and 12 seconds, which corresponds to the period when the fibre optic distance was maintained at 14 cm from the processing zone. During the last 3 seconds of the experiment, the z-stage was adjusted, moving the fibre optic 7 cm closer to the processing zone, resulting an increase in intensity. Since the upper sensitivity level of the spectrometer is 1035 nm, it is not possible to measure the spectra in the NIR and IR regions. Based on these initial experiments, spectroscopy can be regarded as a suitable monitoring system for FLμM. However, in high-speed micromachining, the slow integration time in relation to processing speed might cause a problem.

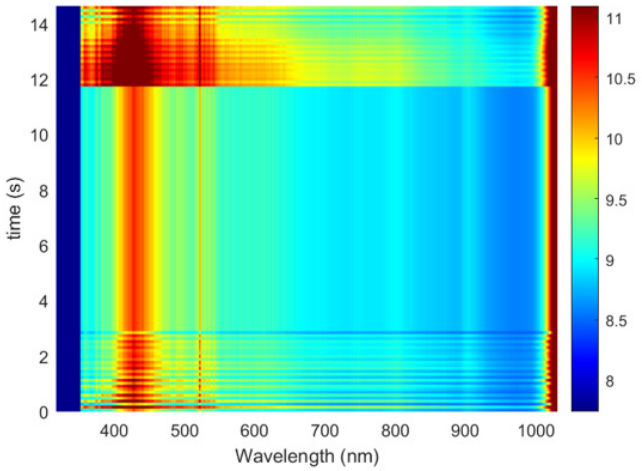

Fig. 4 Collected spectra of 316L steel sample during FLμM of a groove with multiple passes (15 secs total duration).

The electromagnetic emissions obtained during the FLμM process were evaluated to study the impact of the laser energy on the corresponding surface structure. Based on the specific regions identified from the spectrometer (Fig. 4), UPD-based sensors were used to detect the electromagnetic radiations at those wavelengths, which are then converted into and electrical signal response that can be digitalized and analysed. The study focused on two initial cases, selected to allow the direct comparison between the different scenarios and the process response gathered by the photodiode system. During the experiments, to determine the direct relationship between the parameter values and the monitoring signal response, relevant process parameters such as laser pulse energy and number of passes were modified.

During the first part of the experiments to test the compatibility of the measuring system with the fs laser, a con-

stant pulse energy of 25 µJ with two different number of pulses, 10 and 100 pulses were used. Figure 5 shows the measured raw current over time LBR signal of the InGaAs diode during FLµM. The figure depicts the amount of peaks collected corresponding to the amount of pulses sent and the resulting voltage of the photodiode. During the time frame shown in Figure 5, it takes 500 and 5000 µs for the 10 and 100 pulses, respectively. The photodiode signal drops to approximately zero between each pulses and at the end of the experiment. The single-pulse and line experiments (see, Fig. 3) were repeated 5 times to obtain characteristic signature out of the photodiode signal. The data collection system of the FLµM process is sufficiently fast to capture each pulse, but it is not capable of resolving the effects of each pulse at the fs level. Consequently, a plateau is observed at the peak of each pulse as the emissions reach a saturation point where further increases in pulse energy do not increase the intensity. However, the acquisition rate is sufficiently high to monitor the ongoing micromachining process, allowing for precise geometrical information to be collected. Figure 6 shows the resulting SEM images for laser-induced craters using different numbers of pulses at a pulse energy of 25 µJ. It can be clearly seen that deeper craters were produced with 100 pulses in comparison to a shallow craters with 10 pulses.

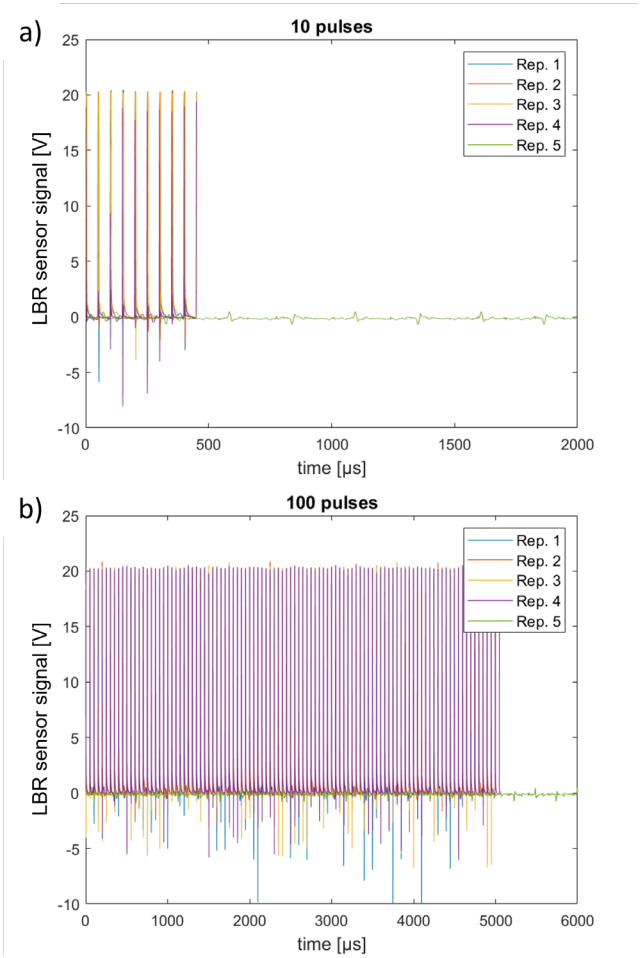

Fig. 5 Corresponding signal response of electromagnetic emissions during FLµM with a) 10 pulses and b) 100 pulses (pulse energy – 25 µJ).

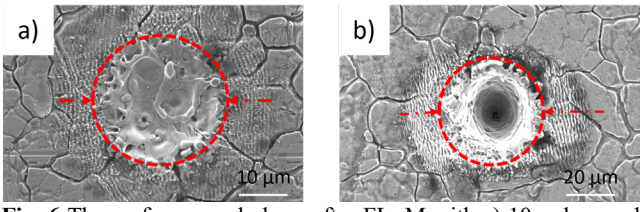

Fig. 6 The surface morphology after FLµM with a) 10 pulses and b) 100 pulses.

In the second part of the experimental design, the effect of various laser parameter such as pulse energy on the structure depth is studied. The captured electromagnetic emissions generated during FLµM using the diode-based monitoring system are shown in Figure 7. Figure 7a shows the signal from the photodiode, which measured the light produced during FLµM. As can be seen here, the signal peaks were obtained whenever there is laser irradiation. The machining of a single groove consists of many laser pulses (20000 pulses). In Figure 7b, a large scale graph of sensor signals is also shown, and a signal peak is repeated every 0.05 ms as the pulse repetition rate was 200 kHz. The time-based statistical comparison of five consecutive passes reveals that the root mean square (RMS) of the intensity trend decreases with an increasing number of laser passes, leading to a greater groove depth (Figure 7c). The sensor signals before and after the peak are symmetric, therefore, the measured signal can be regarded as reliable.

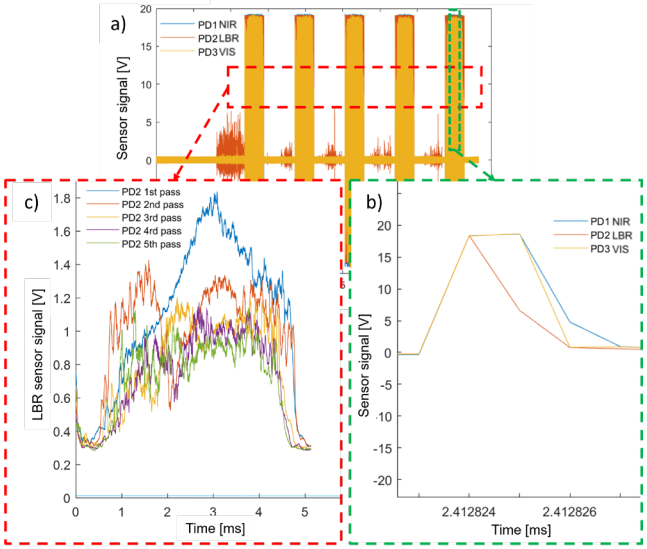

Fig. 7 a) Raw photodiode signal delivered by UPDs during machining of 5 passes of single groove of a 316L plate, b) relationship between the RMS values of the diode intensity and number of laser passes, and, c) emissivity intensity according to various diodes [NIR – Near infrared, LBR – Laser back reflection, VIS – Visible].

Additionally, the recorded time signal is converted into the frequency domain to analyse the relation between the acquired optical emission signals and the laser scanning passes during FLµM. The results of the Fast Fourier Transform (FFT) of the corresponding signals are shown in Figure 8. Based on the signals obtained (Figure 8a), a dominant frequency of 200 kHz and the corresponding harmonics were noticed which can be correlated to the repetition rate of the laser.

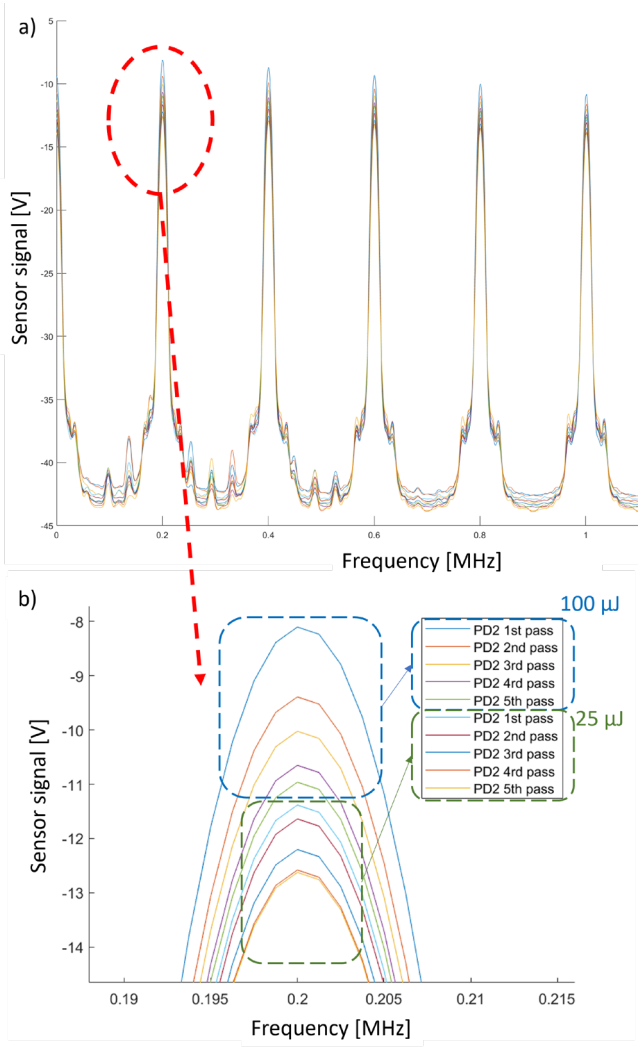

Fig. 8 a) Frequency spectrum of the optical emission signal at different laser scanning passes, b) the correlation between the number of laser passes and the corresponding intensity. 1st to 5th pass of 100 µJ indicated in blue and 1st to 5th pass of 25 µJ indicated in green.

The harmonics of the excitation frequency can be distinguished starting from 200 kHz to 1000 kHz. Notably, the harmonics between 200 – 1000 kHz do not exhibit different behaviour compared to the 0.2, 0.4, 0.6, 0.8 and 1 MHz. The energy of excitation frequency (200 kHz) is shared between the harmonics. Therefore, when each harmonic characteristic is analysed, a similar trend can be seen with decreasing energy. The noise between the harmonics is not as vital as for the OE signal as the signal-to-noise ratio is relatively high. It can be seen from Figure 8b that the machining signal (from the 1st laser pass to the 5th laser pass) can be correlated with the number of laser passes. This graph demonstrates the clear distinction between the machining signal and indicating the feasibility of separating different signal components effectively. The prominent peak at 200 kHz comprises data points from five consecutive laser passes, indicating same pulse repetition rate within experiments. Five distinct peaks are noticeable, decreasing in sensor signal. The FFT-intensity graph demonstrates the sensitivity of the photodiodes in distinguishing individual laser passes. Notably, even with the removal of approximately 1-4 µm of material between each pass, the signal intensity remains discernible.

The quantitative analysis in Figure 9 confirms the inverse relationship between groove depth and LBR emission with high precision. This consistency confirms the reliability of the photodiode signal as a predictor of feature depth under controlled conditions. The inverse relationship implies that deeper grooves might cause light trapping in deeper structures, leading to lower signal intensity. Linear regression yields strong correlation coefficients ($R^2 = 0.99$, $R^2 = 0.99$, $R^2 = 0.98$, and $R^2 = 0.96$ for 100 µJ, 75 µJ, 50 µJ and 25 µJ, respectively), demonstrating a significant linear relationship between the photodiode signal and feature depth. The higher the number of laser passes applied, the lower the intensity of the signals. One portion of the radiation striking the rough and porous surface in the bottom of the groove can diffusively be reflected without reaching the detector. Another portion of the incoming light can be trapped in the cavities of the groove and reflected multiple times within these cavity walls. This guided absorbed light can cause deeper cavities. Consequently, irradiation of the groove resulted in a significant drop in the measured signal. The attenuation in the VIS region needs to be improved, as the plasma-related light emission is insufficiently strong compared to the LBR, causing the process-relevant signal to be suppressed by the system noise.

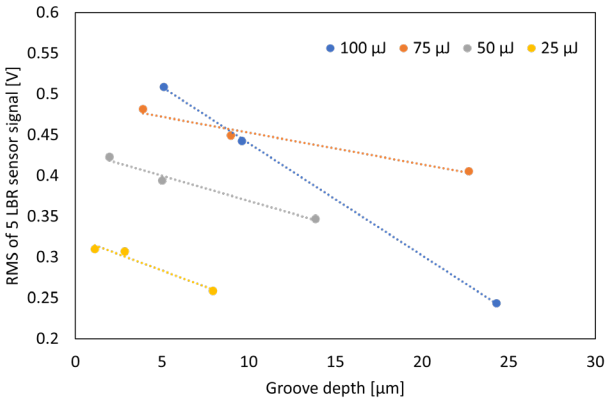

Fig. 9 Average RMS values of optical emissions (LBR) measured from five repeated experiments across the first, third and fifth consecutive laser passes.

4. Conclusions

In this study, an investigation of utilizing optical emissions, originating from the processing zone, for monitoring the FLµM process setup by spectroscopy and ultra-high speed photodiodes was presented. The main conclusions reached after the analysis of the obtained results were:

Spectrometry sensitivity was studied by changing several laser parameters such as number of laser passes and the distance between the process zone and spectroscopy over 15 seconds experiment. The biggest advantage of the spectrometer is to find the process relevant wavelength regions. So far, the spectrometer has been used off-axially, but to get best results from deeper surface structures, it can be implemented coaxially with the laser beam. The measured intensity of the VIS signal was associated with the plasma

formation during the ablation process, whereas the LBR related to the reflected light from the processing region. The decrement of brightness induced by laser is associated with an increase in machining depth. Such method of monitoring of micromachining depth can successfully be applied to different materials and ablation geometries. Experimental results showed that the estimated depths of the laser-induced geometries were inversely proportional to the LBR emission measured, with a high degree of precision. Analysing the FFT spectrum of the recorded signals, it is also possible to monitor the relevant frequencies of the process, namely those associated to the laser repetition rate and scanning of single grooves.

To sum up, this paper shows the potential of ultra-high speed photodiode monitoring for industrial applications as an easy solution to work with monitoring systems. As a result, the proposed method is applicable for ultrashort pulsed lasers as the brightness back reflected light induced by the ultrashort laser is strong enough to collect with ultra-high speed photodiodes. Spectroscopy measurements during running process can help to distinguish which specific spectral ranges of electromagnetic radiations are emitted by the FLμM process.

Acknowledgments

This work was partially funded by the KU Leuven C3 IOF project fs-SPR (C3/20/084) and the Research Foundation - Flanders (FWO-Vlaanderen) Medium-Scale Research Infrastructure project FemtoFac (I001120N).

References

[1] S. Nanthakumar, D. Thangaraju, and R. Kumar: Proc. Inst. Mech. Eng. C. J. Mech. Eng. Sci., 237, (2023) 830.
[2] L. Calabrese, M. Azzolini, F. Bassi, E. Gallus, S. Bocchi, G. Maccarini, G. Pellegrini, and C. Ravasio: J. Manuf. Mater. Process., 5, (2021) 125.
[3] X. Lu, M. D. Wang, P. Zhang, and C. Li: J. Phys. Conf. Ser., 2185, (2022) 012082.
[4] E. Mazur, K. C. Phillips, H. H. Gandhi, and S. K. Sundaram: Adv. Opt. Photonics, 7, (2015) 684.
[5] R. Le Harzic, S. Sommer, D. Breitling, M. Weikert, C. Föhl, C. Valette, C. Donnet, E. Audouard, and F. Dausinger: Appl. Surf. Sci., 249, (2005) 322.
[6] A. Hamad: "Effects of Different Laser Pulse Regimes (Nanosecond, Picosecond and Femtosecond) on the Ablation of Materials for Production of Nanoparticles in Liquid Solution" ed. by R. Viskup **(**IntechOpen, London, UK, 2016) p.305.
[7] J. C. Ion: "Laser processing of Engineering Materials" (Elsevier, Butterworth-Heinemann, Burlington, 2005) p.384.
[8] A. Ostendorf: "3D Laser Microfabrication: Principles and Applications" ed. by H. Misawa and S. Juodkazis (Wiley-VCH Verlag, Weinheim, Germany, 2006) p.341.
[9] E. Glezer, and E. Mazur: Appl. Phys. Lett., 71, (1997) 882.
[10] D. E. Lee, I. Hwang, C. M. O. Valente, J. F. G. Oliveira, and D. A. Dornfeld: Cond. Monit. Control Intell. Manuf., (2006) 33.
[11] W. Wiesemann: "Laser applications" ed. by R. Poprawe, H. Weber, G. Herziger (Springer, Heidelberg, 2004) p.243.
[12] D. Von der Linde and K. Sokolowski-Tinten: Appl. Surf. Sci., 154, (2000) 1.
[13] P. Rußbüldt, T. Mans, M. Hermans, D. Hoffmann, and D. Wortmann: Wiley online Libr., 7, (2010) 41.
[14] R. Schmitt and G. Mallmann: Photonik Int., 11, (2013) 57.
[15] A. Terchi and Y. H. J. Au: Meas. Control, 34, (2001) 240.
[16] P. Verboven, A. Nemeth, M. K. Abera, E. Bongaers, D. Daelemans, P. Estrade, E. Herremans, M. Hertog, W. Saeys, E. Vanstreels, and B. Verlinden: Postharvest Biol. Technol., 78, (2013) 123.
[17] X. Li and Y. Guan: Nanotechnol. Precis. Eng., 3, (2020) 105
[18] M. Grasso and B. M. Colosimo: Meas. Sci. Technol., 28, (2017) 044005.
[19] K. Wasmer, C. Kenel, C. Leinenbach S. A. Shevchik: Industrializing Additive Manufacturing-Proceedings of Additive Manufacturing in Products and Applications-AMPA 2017, (2018) 200.
[20] M. Chen, and M. Lu: Proc. WCMNM 2021, (2001)
[21] M. C. Lu, S. J. Chiou, B. S. Kuo, and M. Z. Chen: Appl. Sci., 11, (2021) 7045.
[22] T. V. Vorburger: Int. J. Adv. Manuf. Technol., 33, (2007) 110.
[23] H. Roozbahani, A. Salminen, M. Manninen: J. Laser Appl., 29, (2017) 022208.
[24] I. Smurov: IV International WLT-Conference on Lasers in Manufacturing 2007, (2007) 537.
[25] J. P. Kruth, J. Duflou, P. Mercelis, J. Van Vaerenbergh, T. Craeghs, and J. De Keuster: Proc. 5th Lane Conf. Laser Assist. Net Shape Eng., 1, (2007) 23.
[26]G. Held: "Introduction to light emitting diode technology and alpplications" (Auerbach publications, New York, USA, 2016) p.53.
[27]D. You, X. Gao, S. Katayama: Sci. Technol. Weld. Join., 19, (2014) 181-201.
[28]S. Postma: "Weld pool control in ND: YAG laser welding" (University of Twente, Twente, 2003) p.43.
[29] W. Duan: J. Opt. Soc. Am. B, 37, (2020) 804.
[30] Y. Park, R. Sehun: Opt. Laser Technol., 39, (2007) 1461.
[31] J. Martan, D. Moskal, L. Prokešová: JLPS-Japan Laser Processing Society, (Osaka, Japan, 2019) 1.
[32] C. Gehrke: "Überwachung der Struktureigenschaften beim Oberflächenstrukturieren mit ultrakurzen Laserpulsen" (Herbert Utz Verlag, München 2013) p.54.
[33] M. Zuric, O. Nottrodt, Peter Abels: J. Laser Micro/Nanoengineering, 14, (2019) 245.
[34] D. Birtalan and W. Nunley: "Optoelectronics" (CRC press, Florida, 2018) p.61.

(Received: June 26, 2024, Accepted: November 17, 2024)